

17 β -Estradiol induces nuclear translocation of CrkL at the window of embryo implantation

Jaya Nautiyal, Pradeep G. Kumar, and Malini Laloraya*

Embryo Implantation Group, Molecular Reproduction Unit, Rm. # 317-319, School of Life Sciences, Devi Ahilya Vishwavidyalaya, Vigyan Bhawan, Khandwa Road Campus, Indore, MP 452017, India

Received 11 March 2004

Abstract

Crk family adaptors are widely expressed and mediate the timely formation of signal transduction protein complexes upon a variety of extracellular stimuli, including various growth and differentiation factors. The window of implantation is the favorable time period when the uterus develops a receptive approach to the invading embryo. Various signaling cascades are likely to become active at the window of implantation both in the uterus and the embryo. This helps create maternal embryo dialogue leading to successful embryo implantation. In this study we report for the first time the presence and nuclear translocation of the adaptor molecule CrkL both in the uterine and embryonic partners at the window of implantation. We also report that estrogen, which initiates and guides crucial changes in the uterus and the embryo at the window of receptivity, causes a massive surge in the expression and subsequent nuclear translocation of CrkL. We have also identified the existence of one LXXLL motif in the CrkL amino acid sequence and a single LXD is sufficient for activation by the estrogen receptor. This is suggestive that CrkL can bind to estrogen receptors and act as a coactivator.

© 2004 Elsevier Inc. All rights reserved.

Keywords: CrkL; Adaptor protein at embryo implantation; Converging signaling pathways; Embryo adhesion; Epithelial mesenchymal transition; LXXLL motif

CrkL (Crk-like), which belongs to the Crk (CT10 regulator of kinase) family of adaptors, is a unique adaptor molecule, which performs diverse roles as a result of being a part of numerous signaling cascades by timely formation of signal transduction protein complexes upon a variety of extracellular stimuli, including various growth and differentiation factors. Selective formation of multiprotein complexes by the Crk and Crk-like (CRKL) proteins depends on specific motifs recognized by their SH2 (Src-homology-2) and SH3 (Src-homology-3) domains. The SH2 domains bind to protein motifs, which usually contain a phosphorylated tyrosine residue followed by specific residues (often in positions +2 and +5). The SH3 domains often bind to proline rich protein motifs and peptides conforming to a core consensus P-x-x-P plus some specificity determining additional residues in the vicinity [1].

Window of receptivity is a state where the events related to cell growth, transformation, differentiation, cellular remodeling, migration, cytoskeletal reorganization, and cell adhesion are very rife. All these phenomena occurring in the uterus call for the activation of various signaling cascades. The adaptor protein CrkL has been implicated in multiple signal transduction pathways. The CrkL(-/-) genotype is partially embryonic lethal [2].

In this study we probe the expression and localization of CrkL, throughout the window of implantation in the mouse uterus and embryo. Implantation in the mouse is initiated as a consequence of an estrogen surge and thus the impact of the ovarian steroids estrogen and progesterone on CrkL expression was also probed. We report that CrkL is profoundly active throughout the window of implantation in both the uterus and the embryo. We also report its nuclear translocation in a stage specific manner in the uterus and the embryo at the window of implantation and under the influence of estrogen, using a delayed implantation model.

* Corresponding author. Fax: +91-731-276-2984.

E-mail address: laloraya@sancharnet.in (M. Laloraya).

Materials and methods

Reagents

Rabbit polyclonal antibodies to CrkL (C-20) sc319, actin (H-196) sc7210, and goat anti-rabbit IgG-HRP sc2030 were from Santa Cruz Biotechnology, USA. Goat anti-rabbit-FITC conjugated antibody was from Bangalore Genie, India. 17β -Estradiol, progesterone, corn oil, diamino benzidine (DAB), hydrogen peroxide (H_2O_2), 2,4,6-diamidino 2-phenyl indole (DAPI), and all other chemicals used for experimentation were purchased from Sigma Chemical (St. Louis, MO, USA). PVDF membrane (0.2 μ m) was purchased from Bio-Rad (Hercules, CA).

Animals

All experiments were performed with SWISS strain mice housed and bred in our animal facility. All animals were given food and water ad libitum and were housed in strict regimens of temperature ($27 \pm 1^\circ C$) and light (14 h light and 10 h dark). All animal protocols were approved by Institutional Review Board.

Two animal models, viz., the pregnant mouse model and the delayed implantation model were used for the experimentation. All experiments on pregnancy and delayed implantation model were performed using 3–4-month-old virgin females.

Pregnancy model. Three to four months old virgin females showing a regular estrus cycle were housed with male mice (3–5 months old), of proven fertility. Mating was checked the following morning by confirming the presence of a vaginal plug and this day was designated as the Day 1 of pregnancy. Pregnant females were sacrificed on early pre-implantation stages Day 4 (10 a.m.), late pre-implantation stage (Day 4, 4 p.m.), peri-implantation (Day 5, 5 a.m.), and late peri-implantation stages (Day 5, 10 a.m.) stages. The uterine tissue was excised, washed in PBS, and flushed for collecting embryos to determine the developmental stage of the embryos in order to stage the time of pregnancy. The uterine tissue was flash-frozen for subsequent experimentation.

Delayed implantation model. Pregnant mice were ovariectomized on Day 3 of pregnancy after 4 p.m. under careful anesthesia prior to the early morning estrogen surge. Two batches of hormonal treatment, viz., A and B were made where A corresponded to progesterone alone treatment while B corresponded to progesterone + estrogen treatment, respectively. Batches A and B were injected with 1 mg/mice/day dose of progesterone subcutaneously starting from the third day after ovariectomy. On the seventh day of pregnancy animals of batch B were subcutaneously injected with 0.1 μ g/mouse dose of estrogen along with 1 mg/mice dose of progesterone while the animals of the progesterone alone batch (A) were injected with 1 mg/mice dose of progesterone only. The animals were sacrificed on the eighth day and the tissue was flash-frozen for further experiments. The uteri of the progesterone alone batch were flushed with PBS into siliconized watch glasses to confirm the presence of unimplanted blastocysts. In the progesterone + estrogen batch the implanted embryo was removed carefully from the uteri by giving a lateral cut in order to avoid any embryonic tissue contamination.

Preparation of cytosolic/nuclear extracts

Uterine tissues for different experimental setups were excised, removed of fat, and washed in PBS (pH 7.4). The tissue was suspended in Buffer A (20 mM Hepes, 10 mM KCl, 1 mM $MgCl_2$, 20% glycerol, 0.1% Triton X-100, 1 mM EDTA, 1 mM DTT, 1 mM sodium orthovanadate, 20 μ M PMSF (pH 7.9), and protease inhibitor tablets (2 tablets/100 ml from Boehringer–Mannheim)) followed by homogenization at 3000 rpm using the polytron homogenizer. The homogenate was incubated on ice on the Genie Rocker-100 for 30 min followed by centrifugation in the Eppendorf 5820R centrifuge at 14,000 rpm at 4°

for 45 min. The supernatant obtained was aspirated and stored as *cytosolic extract* at $-80^\circ C$. The pellet was suspended in chilled Buffer B (Buffer A + 400 mM NaCl) and incubated at room temperature on the rocking shaker for 1 h followed by centrifugation at 14,000 rpm at $4^\circ C$ for 30 min. The aspirated supernatant was the nuclear extract and stored at $-80^\circ C$ for further experimentation.

SDS-PAGE, Western blotting, and immunoblotting

Cytosolic or nuclear proteins were diluted 1:4 with Laemmli sample buffer and equal amount of protein (10 μ g) from each sample was loaded onto an appropriate running gel (pH 8.3) with a 4% stacking gel (pH 6.8). Gels were run on a MiniProtein III vertical electrophoresis system (Bio-Rad) at 100 V for 3 h. The separated proteins were transferred onto Sequiblot PVDF (0.2 μ m, Bio-Rad) in transfer buffer [25 mM Tris, 190 mM glycine (pH 8.2), and 40% methanol (v/v)] using a Mini Transblot cell (Bio-Rad) at 15 mA constant current for each membrane for 12–16 h.

The blots were pre-wet in methanol, washed thrice (5 min each) in phosphate-buffered saline (PBS) with 0.1% Tween 20, followed by blocking (5% non-fat milk) for 60 min at RT with gentle shaking. The membranes were washed five times in PBS-T and incubated for 1 h at 1:1000 dilution of Rabbit polyclonal CrkL primary antibody. Peroxidase conjugated goat anti-rabbit IgG (Santa Cruz Biotechnology) was then added as the secondary antibody. Immunopositive bands were detected using the color development method employing the DAB/ $NiCl_2/H_2O_2$ reaction. Images were captured on a Chemi-imager from the Alpha Innotech, USA. Signal quantification was performed by the Phoretix 1D Advanced Version 5.20, software by the Alpha Innotech, USA.

Immunocytochemistry of the uterine sections

Uterine tissues of different experimental models were processed and sectioned as detailed earlier [3]. The slides were microwaved in 10 mM citrate buffer (10 mM sodium citrate, 10 mM citric acid, pH 6) for 2 min. The slides were processed and incubated overnight in 1:200 diluted CrkL primary antibody at $4^\circ C$ in a humid chamber. Slides were subsequently rinsed in phosphate-buffered saline (10 mM, pH 7.4) and incubated with 1:200 dilution of goat anti rabbit secondary antibody (BG-FTC-2, Bangalore Genie) for 2 h. They were further processed for nuclear staining by incubating in 1:1000 dilution of 1 mg/ml solution of 4',6-diamidino-2-phenylindole-dihydrochloride hydrate (DAPI) for 10 min. The results were observed under a Nikon Epi-fluorescence microscope and the images were captured by the Cool Snap Camera and the Documentation System from the Alpha Innotech, USA.

Blastocyst collection and immunostaining

The uteri excised from the different stages of pregnancy model were flushed with PBS into siliconized watch glasses in order to bring out the embryo. The watch glasses were observed under the microscope to check for the presence of right staged embryos. The embryos were fixed in 4% paraformaldehyde (filtered) followed by neutralization with 50 mM NH_4Cl and subsequent permeabilization with 0.25% Triton X-100. Each step was mediated by careful washing with PBST. The embryos were blocked in 5% normal goat serum in PBS (filtered) followed by overnight incubation with 1:200 diluted CrkL primary antibody at $4^\circ C$. The following day the embryos were washed and then incubated with FITC-conjugated 1:200 diluted goat anti rabbit secondary antibody (BG-FTC-2, Bangalore Genie) for 1 h. The embryos were processed for nuclear staining as detailed in the earlier section by incubation with DAPI (1:1000) for 10 min prior to observation under the microscope. The reaction was stopped by subsequent washings. The embryos were observed under the Nikon microscope followed by image capturing with the Cool Snap camera.

Statistical analysis

All the experiments were repeated five times from five separate individuals. Western blots were digitized on a Chemimager 4400 (Alpha Innotech, CA). Band volumes were integrated using Phoretix 1-D image analysis software (version 5.20, Nonlinear Dynamics, NC, USA). The data were subjected to a two-tailed *T* test.

Results

CrkL expression in the uterus at the window of receptivity

We examined the expression profile of CrkL in the uterine cytosolic and nuclear extracts at the window of receptivity using the Western blot analysis. Same levels of protein concentration were maintained in all the lanes as demonstrated by the actin immunoblot for the subsequent protein lanes (Fig. 1A).

Our Western blot data demonstrated that a decrease in the CrkL expression, in the cytosol through the different stages of the window of receptivity starting from Day 4 (10 a.m.), a stage outside the window of receptivity, is evident (Fig. 1B). The decrease was gradual from Day 4 (10 a.m.) to Day 5 (5 a.m.) because the levels of CrkL at the Day 4 (10 a.m.) were not significantly different from the Day 4 (4 p.m.) and Day 5 (5 a.m.). The decrease in CrkL expression between Day 4 (4 p.m.) stage and Day 5 (5 a.m.) stage is not significant. A sudden decrease in the CrkL expression in the cytosolic samples at the Day 5 (10 a.m.) stage is evident and this decline was highly significant when compared with Day 4 (10 a.m.), pre-receptive stage ($p < 9.22 \times 10^{-5}$;

Day 4 (4 p.m.), late pre-implantation stage ($p < 0.0008$); and Day 5 (5 a.m.) peri-implantation stage ($p < 0.0001$).

The CrkL expression in the corresponding nuclear extracts on Western blots and their corresponding histogram (Figs. 1A and B) demonstrates a continuous increasing trend starting from Day 4 (10 a.m.) to Day 5 (10 a.m.) stages through the Day 4 (4 p.m.) and Day 5 (5 a.m.) stages. A very significant increase characterizes the Day 4 (4 p.m.) stage when compared to Day 4 (10 a.m.) stage ($p < 0.0005$), the Day 5 (5 a.m.) stage as opposed to Day 4 (10 a.m.) ($p < 0.005$), and Day 4 (4 p.m.) stage ($p < 0.03$). Similar elevated levels of CrkL were maintained at the Day 5 (5 a.m.) and Day 5 (10 a.m.) nuclear extracts. The levels of CrkL were significantly higher at the late peri-implantation Day 5 (10 a.m.) stage, when compared to the Day 4 (10 a.m.) stage ($p < 0.03$).

A calculation of the nuclear to cytosolic ratio and the percentage of nuclear translocation (Figs. 1A and C) demonstrated that a tremendous increase in the nuclear to cytosolic ratio and percentage of nuclear translocation values as the uterus proceeded from the Day 4 (10 a.m.) stage to the Day 5 (10 a.m.) stage through the Day 4 (4 p.m.), and Day 5 (5 a.m.) stage. The lowest values were present at the Day 4 (10 a.m.) (0.03, 16.06%) pre-receptive stage while the highest values of nuc/cyt ratio and percentage of nuclear translocation were present at the Day 5 (10 a.m.), post-implantation stage (30.21, 97.07%).

The immunolocalization of CrkL on the uterine tissue sections is shown in Fig. 2. The panel on the right is the DAPI stained image reflecting nuclear staining to understand the spatio-temporal distribution of CrkL in the

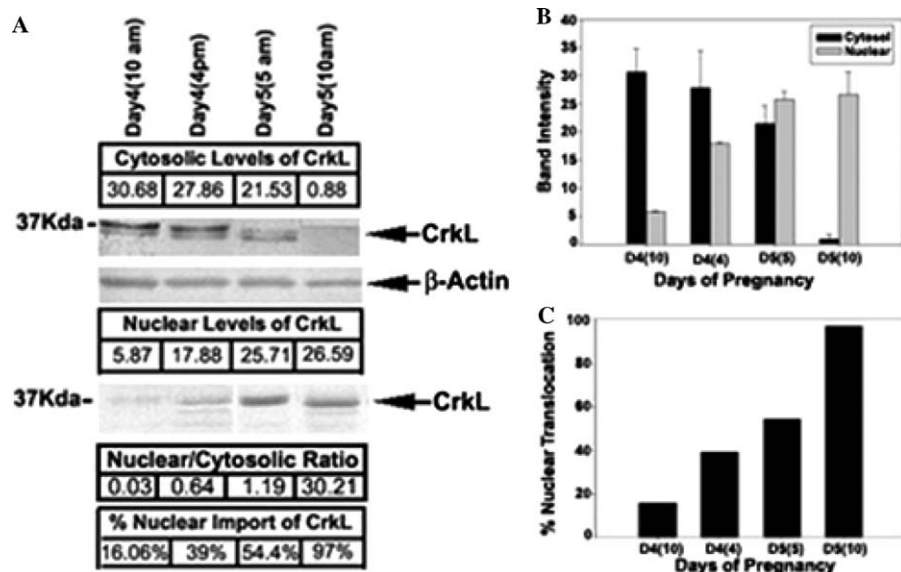


Fig. 1. Western blot analysis of CrkL expression in the uterus at the window of receptivity. (A) Image showing CrkL levels in the cytosolic and nuclear extracts, as the uterus proceeds through the nonreceptive, Day 4 (10 a.m.) stage to the different stages of window of receptivity, i.e., Day 4 (4 p.m.) pre-implantation, Day 5 (5 a.m.), peri-implantation, and Day 5 (10 a.m.) late peri-implantation. (B) Histogram of CrkL expression in cytosolic and nuclear extracts during early pregnancy while (C) is a bar diagram of the nuclear translocation percentage.

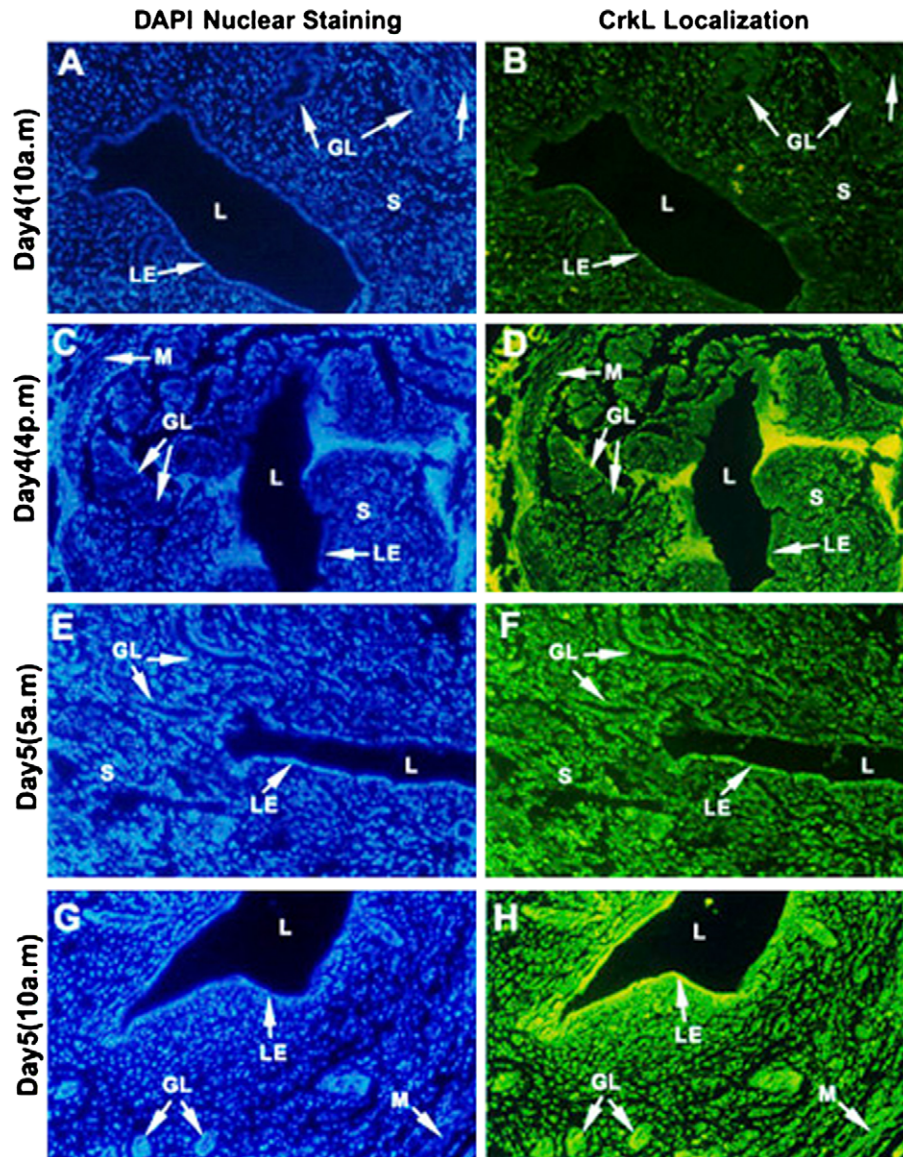


Fig. 2. Immunocytochemical localization of CrkL in the uterus at the window of receptivity. Image shows the changing localization and levels of expression of CrkL as the uterus moves from the Day 4 (10 a.m.) nonreceptive stage (B) to the different stages of window of receptivity, i.e., Day 4 (4 p.m.) late pre-implantation (D), Day 5 (5 a.m.) peri-implantation (F), and Day 5 (10 a.m.) late peri-implantation (H) stages while (A), (C), (E), and (G) represent respective DAPI staining. L, lumen; LE, luminal epithelium, S, stroma; M, myometrium; GL, glands; GE, glandular epithelium. 50× magnification.

uterus. At the Day 4 (10 a.m.) stage, localization was observed on the luminal epithelium and stroma but the quantitative expression of CrkL was very less at this stage. A comparison with the corresponding DAPI image which demonstrated the nuclei on the whole tissue sections revealed that relatively lesser nuclear levels of CrkL were present. At the Day 4 (4 p.m.) stage (late pre-implantation stage) a quantitative increase in the CrkL expression is observed. Expression was mainly localized on the stroma and the myometrium. Some patches of expression were also seen on the luminal epithelium. A comparison with the corresponding DAPI image demonstrated that there was a shift towards a nuclear localization of CrkL at this stage.

Elevated CrkL expression characterizes Day 5 (5 a.m.) stage with the expression chiefly localized on the stroma, glands, and the luminal epithelium. A comparison with the DAPI image demonstrated that tangible levels of nuclear translocation of CrkL were present at this stage. At the Day 5 (10 a.m.) late peri-implantation stage there was very heavy localization on the stromal cells, luminal epithelium, and glands. A comparison of the fluorescence image and the DAPI image revealed that the fluorescence image of the CrkL localization was exactly similar to the DAPI image. As can be observed from the images maximum nuclear translocation of CrkL was observed at the Day 5 (10 a.m.) stage.

CrkL localization on the embryo

The localization of CrkL on the different stages of the mouse embryo at the window of implantation has been

shown in Fig. 3. The image demonstrates the immunolocalization of the CrkL on the Day 4 (10 a.m.) embryos and its corresponding DAPI images to judge whether it reveals the nuclear or cytosolic distribution. The Day 4

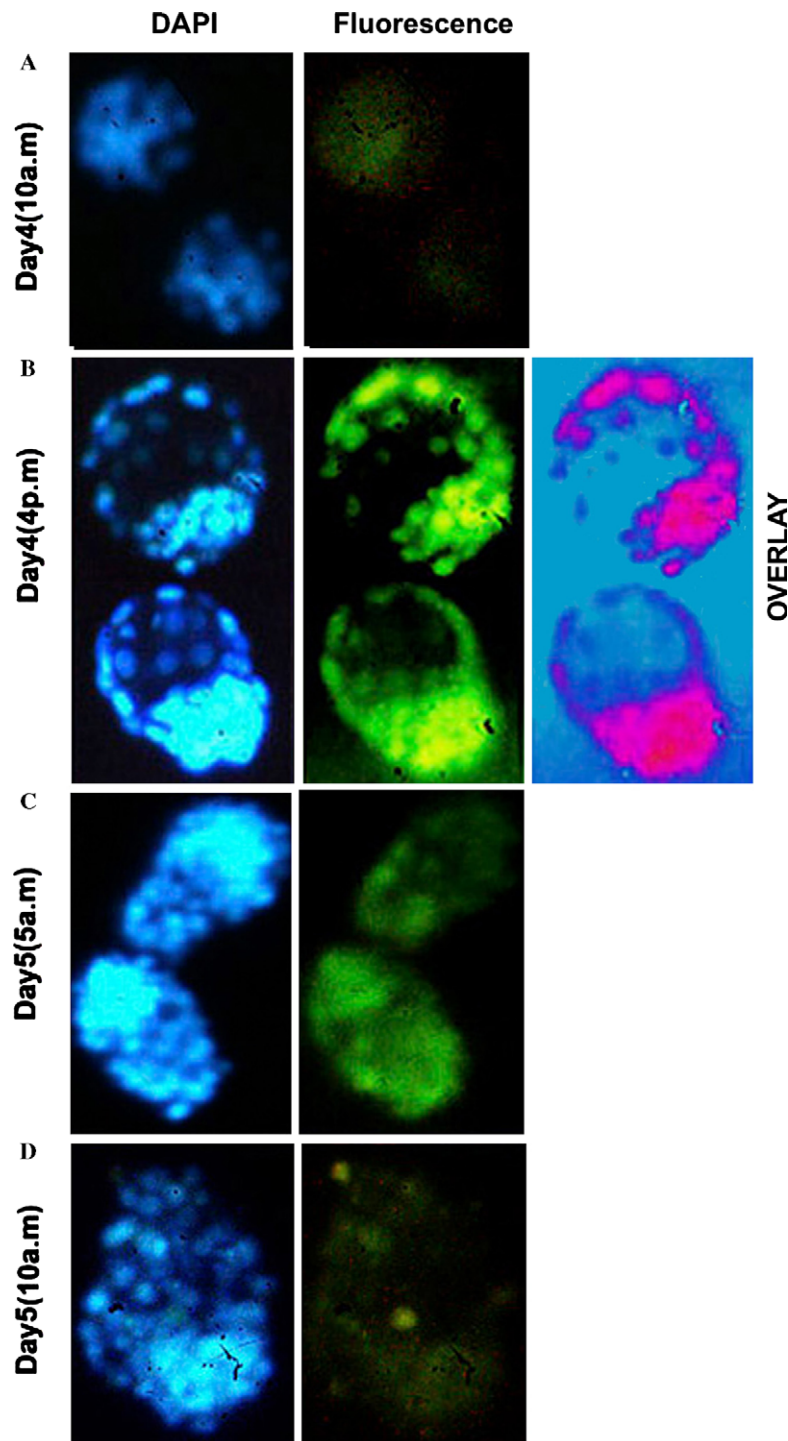


Fig. 3. Immunocytochemical localization of CrkL on the embryo at the window of receptivity. The image on the left of each panel denotes the DAPI stained image highlighting the nuclei of the embryos. The CrkL localization is represented by the fluorescence image towards the right. Image shows the distribution and distribution of CrkL at the Day 4 (10 a.m.) pre-receptive stage (A), Day 4 (4 p.m.) late pre-implantation stage (B), Day 5 (5 a.m.) peri-implantation stage (C), and Day 5 (10 a.m.) late peri-implantation stage (D). The image on the extreme right represents a merger of the DAPI stained and fluorescence image of the embryos. The areas of overlap are represented in magenta (CrkL). 100 \times magnification. (For interpretation of the references to colour in this figure legend, the reader is referred to the web version of this paper.)

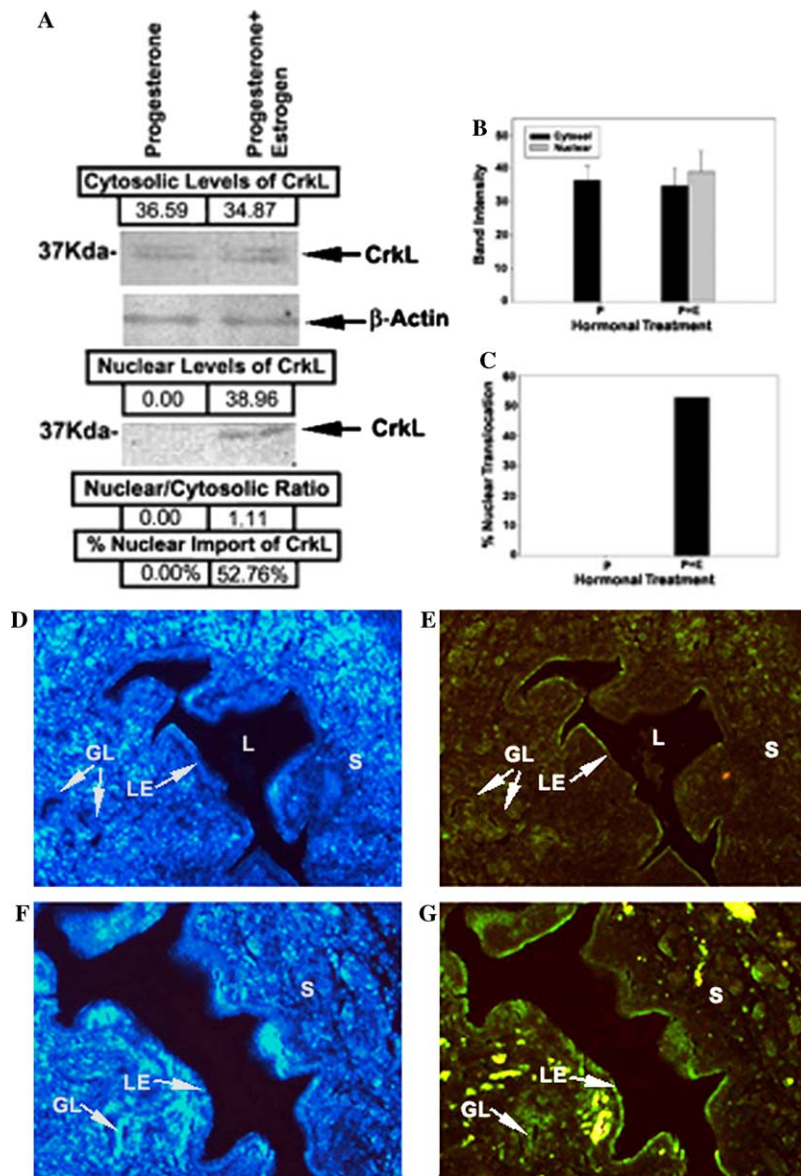


Fig. 4. Western blot analysis of the hormonal effect on CrkL in the uterus using the delayed implantation model: Western blot image showing CrkL levels in the cytosolic and nuclear extracts, in the uterus under the influence of progesterone alone and progesterone + estrogen treatment in the delayed implantation model. The results of (A) are represented as a histogram with error bars (B). Histogram depicting the percentage of nuclear translocation of CrkL under estradiol influence is represented in (C). Image shows spatiotemporal distribution of CrkL under the influence of progesterone alone (E) and progesterone + estrogen (G) while (D) and (F) are the respective DAPI images. L, lumen; LE, luminal epithelium; S, stroma; and GL, glands. 50× magnification.

(10 a.m.) embryos were weakly immunopositive for the CrkL expression with the expression predominantly cytosolic (Fig. 3A). The Day 4 (4 p.m.) embryos reveal intense fluorescence with massive nuclear appearance on the inner cell mass cells and the trophectoderm (Fig. 3B). This was confirmed by a comparison of the DAPI and the fluorescence image (FL) of the CrkL immunolocalization. The two images were so similar that they could be 100% merged. The merged image has been shown as one on the extreme right of Fig. 3B. The magenta color signifies the regions of overlap of the DAPI and the FL image and the intensity of the color is directly proportional to the density

of the cells. Moderate cytosolic as well as nuclear CrkL expression was observed on the embryos of the Day 5 (5 a.m.) stage (Fig. 3C) while the Day 5 (10 a.m.) embryos revealed diminished CrkL expression (Fig. 3D). The expression at this stage was also cytosolic with a very less dotted appearance suggesting the absence of CrkL in the nucleus.

CrkL expression under the influence of ovarian steroids in the delayed implantation model

Western blots were performed using the cytosolic and nuclear samples of the hormone treated delayed

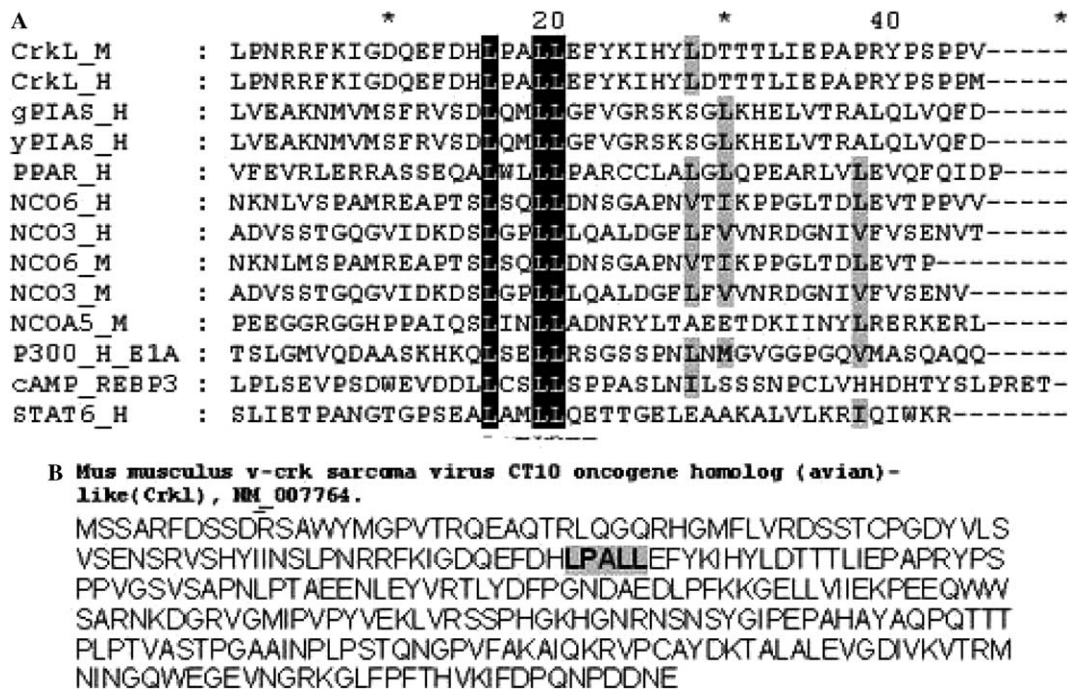


Fig. 5. Genedoc alignment of LXXLL motif in CrkL and established LXXLL motif containing proteins which bind Nuclear receptors (A). CrkL is shown to contain a single LXXLL motif in its amino acid sequence (B).

implantation batches, viz., progesterone alone and progesterone + estrogen using the CrkL polyclonal antiserum. The actin blot in the panel depicts equal protein levels, Fig. 4A. Almost similar levels of CrkL were present in the cytosolic extracts in both the progesterone alone and progesterone + estrogen batches. There was no presence of CrkL in the nuclear extracts of the progesterone alone batch while significant CrkL presence was observed in the progesterone + estrogen batch in the nuclear extracts ($p < 0.003$). The total levels of CrkL were much elevated in the progesterone + estrogen batch when compared to progesterone alone batch (Fig. 4B). There was no nuclear translocation of CrkL in the progesterone alone batch while increased nuclear translocation with the estrogen treatment was evident (Fig. 4C).

The immunocytochemical localization of CrkL in the progesterone alone samples and progesterone + estrogen samples was probed. The results (Fig. 4) show that the CrkL levels in the progesterone alone batch (E) were negligible when compared to progesterone + estrogen batches (G). A weak immunofluorescence was restricted mainly to the luminal epithelium in the progesterone alone batch. Faint expression was seen on the glands, the stroma, and the glandular epithelium. In the progesterone + estrogen batch there was an increased significant CrkL localization with the immunofluorescence restricted to luminal epithelium and stroma (Fig. 4G).

Identification of LXXLL motif in CrkL

Analysis of the sequence of CrkL available in the GenBank (NM_007764) revealed the presence of one LXXLL motif in this protein. A genedoc alignment of CrkL sequence with classical LXXLL domain containing proteins around the area of the LXXLL motif is presented in Fig. 5. The GenBank accession details for the sequences used are as follows: crkL_M (NM_007764); CrkL human (NM_005207); gPIAS_H (Q8N2W9); yPIAS_H (NP_056981); PPAR_H (Q9BYK8); NCO6_H (Q14686); NCO3_H (Q9Y6Q9); NCO6_M (Q9JL19); NCO3_M (O09000); NCoA5_M (Q91W39); P300_H E1A (Q09472); cAMP REBP3_H (NP_006359); and STAT6_H (NP_003144).

Discussion

Our results demonstrate a prominent presence of CrkL both in the cytosol and nucleus, in a stage specific manner in the uterus and the embryo as shown by our Western blot and immunocytochemistry data. 17β -Estradiol induces nuclear translocation of CrkL in the uterus as evidenced by delayed implantation model.

The central event in embryo implantation is the formation of a morphologically and functionally specialized cell-cell contact between the endometrium and the blastocyst through the two simple epithelia, i.e., the

uterine epithelia and the trophectoderm. Because, simple epithelia bear a polarized character, the fact that at the window of receptivity the uterine epithelium and the trophectoderm interact through the apical surface renders the phenomenon of implantation a cell biological paradox [4–7]. It is now known that during the window of implantation there a characteristic epithelial–mesenchymal transition which is active. The epithelial–mesenchymal (EM) transition [8] has been implicated in morphogenesis and tissue remodeling during development [9]. CrkL has been demonstrated to promote epithelial–mesenchymal like transition and promotes cell spreading and breakdown of adherens junctions in MDCK, breast cell line, and cell dispersal in well-differentiated breast carcinoma cells [10]. We hypothesize that the CrkL expressed at the “window of implantation,” might be actively involved in the E–M transition, which takes place at the window of receptivity.

Several growth factors and their receptors have been found to be localized on the uteri and embryo at the window of receptivity. The epidermal growth factor family and their receptors (Erbs) have been reported in the uterus and embryo at the peri-implantation period and they could be playing many crucial roles at this time point which could include embryo uterine interactions [11,12]. The downstream mechanism of signaling of the growth factors at the window of receptivity is still to be elucidated. CrkL has been reported to be activated downstream to epidermal growth factor signaling via the EGF receptor in human mammary epithelial cells [13]. Many other studies have shown that the Crk family of proteins play an important role in growth factor stimulated signal transduction [14,15]. Thus, the CrkL presence at the window of receptivity could be a result of an active growth factor signaling prevalent in the uterus at the window of receptivity.

The *integrins* are among the best characterized immunohistochemical markers of uterine receptivity [16]. These glycoproteins serve as receptors for a variety of extracellular matrix ligands and act as modulators of cellular function through both attachment and signal transduction [17]. The extracellular matrix exerts profound control over cells specifically at the time of window of implantation [18]. The cells interact with the ECM proteins such as fibronectin, laminin, and vitronectin at the *focal adhesions* through the integrins [19]. At the focal adhesions many cytoskeletal proteins and signaling molecules get integrated. Crk proteins are also known to be constitutively associated with effector molecules that mediate cell adhesion. When the signals from the extracellular matrix are received by the integrins to cause their stimulation, this elicits the tyrosine phosphorylation of several proteins in the focal adhesions which include Fak (focal adhesion kinase) [20], paxillin [21], tensin [22], and Cas [23] which interact with CrkL downstream in the transmission of their respective signals [1].

Upon integrin stimulation the focal adhesion kinases and Src cooperate to phosphorylate Cas (Crk associated substrate) [24,25]. Cas is a major CrkL binding protein and thus CrkL is activated downstream to the integrin signaling, which is very active at the window of implantation and specifically at the time of decidualization. Decidualized endometrial stromal cells display alteration of integrins at the time of implantation [26,27]. CrkL activates integrin-mediated hematopoietic cell adhesion [28]. Thus, the presence of CrkL at the window of receptivity and its localization mainly on the stroma when the integrin-mediated interactions of the stromal cells with the extracellular matrix may aid in the stromal cell transformation into decidual cells during the peri-implantation and post-implantation stages is also a very sound possibility.

The signaling by the Src family kinases (SFKs) is also crucial for embryonic development. A triple mutation in Src, Yes, and Fyn, three members of the Src family kinases, leads to severe developmental defects and lethality by E9.5 [29]. The Src family members further recruit CrkL in their downstream signaling cascades. Hence, the active presence of CrkL on the mouse embryo could mean that CrkL is involved in regulating crucial developmental programs in the embryo. Mice homozygous for a targeted null mutation at the CrkL locus exhibited defects in multiple cranial and cardiac neural crest derivatives including the cranial ganglia, aortic arch arteries, cranial outflow tract, thymus, parathyroid glands, and craniofacial structures. These defects indicate an essential stage and tissue specific role for CrkL in differentiation and survival of the neural crest cells during development [30].

CrkL is also an established nuclear adaptor. CrkL is known to bind Stat5 and translocate with it into the nucleus in order to regulate the STAT regulated genes under Type I interferons (IFN- α) [31]. Thrombopoietin induces association of CrkL with STAT5 but not STAT3 in human platelets and CrkL is a component of the nuclear DNA binding complex [32]. CrkL functions as a nuclear adaptor protein that can associate with and activate Stat proteins in Bcr-Abl-expressing cells [33]. Both Stat5a and Stat5b migrate into the nucleus both in the uterus and embryo at the window of receptivity (unpublished observation). Thus, our results showing existence of CrkL in the nucleus are suggestive that CrkL could be a part of the STAT DNA binding complex. We propose a possible convergence of the CrkL–Stat5 signaling pathways at the window of implantation.

Steroid hormone receptors (SHRs) are members of the superfamily of ligand-activated transcription factors that regulate many biological processes. Co-regulators act as bridging molecules between the SHR and general transcription factors to enhance transactivation of target genes [34]. Ligand-dependent activation of gene transcription by nuclear receptors is dependent on the

recruitment of coactivators, including a family of related NCoA/SRC factors, via a region containing three helical domains sharing an LXXLL core consensus sequence, referred to as LXD. Receptor-specific differential utilization of LXXLL-containing motifs of the NCoA-1/SRC-1 coactivator has been established. Whereas a single LXD is sufficient for activation by the estrogen receptor, different combinations of two, appropriately spaced, LXDs are required for actions of the thyroid hormone, retinoic acid, peroxisome proliferator-activated, or progesterone receptors. The specificity of LXD usage in the cell appears to be dictated, at least in part, by specific amino acids carboxy-terminal to the core LXXLL motif that may make differential contacts with helices 1 and 3 (or 3') in receptor ligand-binding domains. Intriguingly, distinct carboxy-terminal amino acids are required for PPAR γ activation in response to different ligands. Related LXXLL-containing motifs in NCoA-1/SRC-1 are also required for a functional interaction with CBP, potentially interacting with a hydrophobic binding pocket [35]. Thus, the LXXLL-containing motifs have evolved to serve overlapping roles that are likely to permit both receptor-specific and ligand-specific assembly of a coactivator complex, and that these recognition motifs underlie the recruitment of coactivator complexes required for nuclear receptor function.

The importance of LXXLL motif is shown in action of peroxisome proliferator-activated receptor- γ (PPAR- γ)—a ligand-dependent transcription factor which depends on interactions with co-activators, including steroid receptor co-activating factor-1 (SRC-1). Glutamate and lysine residues that are highly conserved in LBDs of nuclear receptors form a 'charge clamp' that contacts backbone atoms of the LXXLL helices of SRC-1 and two consecutive LXXLL motifs of SRC-1 make identical contacts with both subunits of a PPAR- γ homodimer [36]. Nuclear factor- κ B (NF- κ B) recruits a coactivator complex that has striking similarities to that recruited by nuclear receptors. Like nuclear receptor-dependent gene expression, NF- κ B-dependent gene expression requires specific LXXLL motifs in one of the p160 family members [37]. The importance of LXXLL motif is also known for retinoic-acid receptor- α (RAR- α) [38].

The window of receptivity is tightly regulated by estrogen surge which occurs before the peri-implantation stage in a background of progesterone and opens the window of receptivity which is crucial for embryo implantation in mice [39]. Studies on the delayed implantation model revealed a 17 β -estradiol inducible increased expression of CrkL levels and increased nuclear translocation of CrkL. The presence of a single LXXLL motif in CrkL is suggestive of its role as a co-activator of estrogen receptor under estrogen action since a single LXXLL motif is sufficient for activation by the estrogen receptor (Fig. 5). This argument appears

to explain nuclear translocation of CrkL under the influence of estrogen.

Thus, CrkL which encompasses a LXXLL motif could be an important mediator of estrogen-dependent signaling. CrkL could serve as an adaptor for integrin and/or growth factor-mediated signaling forming the platform for these crucial signaling cascades. CrkLs export to the nucleus could serve as a marker for embryo activation. A study on CrkL expression in infertility cases would reveal important signature pattern differences from the normal fertility cases.

Acknowledgments

This work was partially supported by a grant from Department of Science and Technology, India, to Dr. Malini Laloraya vide Sanction No. SP/SO/C-51/2000. J.N. was supported by a Senior Research Fellowship from the CSIR (# 9/301(97)/2002 EMRI).

References

- [1] S.M. Feller, *Oncogene* 20 (2001) 6348–6371.
- [2] A.C. Peterson, R.E. Marks, P.E. Fields, A. Imamoto, T.F. Gajewski, *Eur. J. Immunol.* 33 (2003) 2687–2695.
- [3] D. Saxena, S.B. Purohit, G.P. Kumer, M. Laloraya, *Nitric Oxide* 4 (2000) 384–391.
- [4] H.W. Denker, *J. Exp. Zool.* 266 (1993) 541–558.
- [5] H.W. Denker, *Anat. Anz.* 176 (1994) 53–60.
- [6] H.W. Denker, M. Thie, *Ital. J. Anat. Embryol.* 106 (2001) 291–306.
- [7] X. Li, A. Warri, S. Makela, T. Ahonen, T. Streng, R. Santti, M. Poutanen, *Endocrinology* 143 (2002) 4074–4083.
- [8] J.L. Carsol, S. Gingras, J. Simard, *Mol. Endocrinol.* 16 (2002) 1696–1710.
- [9] G. Riedlinger, R. Okagaki, K.U. Wagner, E.B. Rucker III, T. Oka, K. Miyoshi, J.A. Flaws, L. Hennighausen, *Biol. Reprod.* 66 (2002) 438–444.
- [10] L. Lamorte, I. Royal, M. Naujokas, M. Park, *Mol. Biol. Cell* 13 (2002) 1449–1461.
- [11] H. Lim, S.K. Dey, S.K. Das, *Endocrinology* 138 (1997) 1328–1337.
- [12] B.C. Paria, H. Lim, S.K. Das, J. Reese, S.K. Dey, *Semin. Cell Dev. Biol.* 11 (2000) 67–76.
- [13] H. Yamashita, M.T. Nevalainen, J. Xu, M.J. LeBaron, K.U. Wagner, R.A. Erwin, J.M. Harmon, L. Hennighausen, R.A. Kirken, H. Rui, *Mol. Cell. Endocrinol.* 183 (2001) 151–163.
- [14] M.I. Gallego, N. Binart, G.W. Robinson, R. Okagaki, K.T. Coschigano, J. Perry, J.J. Kopchick, T. Oka, P.A. Kelly, L. Hennighausen, *Dev. Biol.* 229 (2001) 163–175.
- [15] L. Hennighausen, G.W. Robinson, K.U. Wagner, X. Liu, *J. Mamm. Gland. Biol. Neoplasia* 2 (1997) 365–372.
- [16] B.A. Lessey, *Hum. Reprod.* 13 (Suppl. 3) (1998) 247–258, discussion 259–261, 247–258.
- [17] W. Doppler, M. Windegg, C. Soratroi, J. Tomasi, J. Lechner, S. Rusconi, A.C. Cato, T. Almlof, J. Liden, S. Okret, J.A. Gustafsson, H. Richard-Foy, D.B. Starr, H. Klocker, D. Edwards, S. Geymayer, *Mol. Cell. Biol.* 21 (2001) 3266–3279.
- [18] D.P. Edwards, S.A. Leonhardt, E. Gass-Handel, *J. Soc. Gynecol. Invest.* 7 (2000) S22–S24.
- [19] P. Dentelli, L. Del Sorbo, A. Rosso, A. Molinar, G. Garbarino, G. Camussi, L. Pegoraro, M.F. Brizzi, *J. Immunol.* 163 (1999) 2151–2159.

- [20] C.A. Lange, J.K. Richer, K.B. Horwitz, *Mol. Endocrinol.* 13 (1999) 829–836.
- [21] J.K. Richer, C.A. Lange, N.G. Manning, G. Owen, R. Powell, K.B. Horwitz, *J. Biol. Chem.* 20 (273) (1998) 31317–31326.
- [22] C.A. Lange, J.K. Richer, T. Shen, K.B. Horwitz, *J. Biol. Chem.* 20 (273) (1998) 31308–31316.
- [23] G.A. Jahn, N. Daniel, G. Jolivet, L. Belair, C. Bole-Feysot, P.A. Kelly, J. Djiane, *Biol. Reprod.* 57 (1997) 894–900.
- [24] P.J. Ruest, N.Y. Shin, T.R. Polte, X. Zhang, S.K. Hanks, *Mol. Cell. Biol.* 21 (2001) 7641–7652.
- [25] F.A. Feltus, B. Groner, M.H. Melner, *Mol. Endocrinol.* 13 (1999) 1084–1093.
- [26] B.A. Lessey, A.J. Castelbaum, C.A. Buck, Y. Lei, C.W. Yowell, J. Sun, *Fertil. Steril.* 62 (1994) 497–506.
- [27] P. Ruck, K. Marzusch, E. Kaiserling, H.P. Horny, J. Dietl, A. Geiselhart, R. Handgretinger, C.W. Redman, *Lab. Invest.* 71 (1994) 94–101.
- [28] A. Arai, Y. Nosaka, H. Kohsaka, N. Miyasaka, O. Miura, *Blood* 93 (1999) 3713–3722.
- [29] L. Zhong, T.G. Parmer, M.C. Robertson, G. Gibori, *Biochem. Biophys. Res. Commun.* 235 (1997) 587–592.
- [30] H. Pendeille, N. Carpino, J.C. Marine, Y. Takahashi, M. Muller, J.A. Martial, J.L. Cleveland, *Mol. Cell. Biol.* 21 (2001) 6549–6558.
- [31] E.N. Fish, S. Uddin, M. Korkmaz, B. Majchrzak, B.J. Druker, L.C. Platanias, *J. Biol. Chem.* 274 (1999) 571–573.
- [32] K. Ozaki, A. Oda, H. Wakao, J. Rhodes, B.J. Druker, A. Ishida, M. Wakui, S. Okamoto, K. Morita, M. Handa, N. Komatsu, H. Ohashi, A. Miyajima, Y. Ikeda, *Blood* 92 (1998) 4652–4662.
- [33] J. Rhodes, R.D. York, D. Tara, K. Tajinda, B.J. Druker, *Exp. Hematol.* 28 (2000) 305–310.
- [34] F. De Miguel, S.O. Lee, S.A. Onate, A.C. Gao, *Nucl. Recept.* 1 (2003) 3.
- [35] E.M. McInerney, D.W. Rose, S.E. Flynn, S. Westin, T.M. Mullen, A. Krones, J. Inostroza, J. Torchia, R.T. Nolte, N. Assa-Munt, M.V. Milburn, C.K. Glass, M.G. Rosenfeld, *Genes Dev.* 12 (1998) 3357–3368.
- [36] R.T. Nolte, G.B. Wisely, S. Westin, J.E. Cobb, M.H. Lambert, R. Kurokawa, M.G. Rosenfeld, T.M. Willson, C.K. Glass, M.V. Milburn, *Nature* 395 (1998) 137–143.
- [37] K.A. Sheppard, D.W. Rose, Z.K. Haque, R. Kurokawa, E. McInerney, S. Westin, D. Thanos, M.G. Rosenfeld, C.K. Glass, T. Collins, *Mol. Cell. Biol.* 19 (1999) 6367–6378.
- [38] S. Westin, R. Kurokawa, R.T. Nolte, G.B. Wisely, E.M. McInerney, D.W. Rose, M.V. Milburn, M.G. Rosenfeld, C.K. Glass, *Nature* 395 (1998) 199–202.
- [39] H. Lim, H. Song, B.C. Paria, J. Reese, S.K. Das, S.K. Dey, *Vitam. Horm.* 64 (2002) 43–76.